The EMBO Journal Vol.16 No.13 pp.3822–3832, 1997

Glutamate transporter EAAC-1-deficient mice develop dicarboxylic aminoaciduria and behavioral abnormalities but no neurodegeneration

Pietro Peghini, Julia Janzen and Wilhelm Stoffel[1]

Laboratory of Molecular Neuroscience, Institute of Biochemistry, Faculty of Medicine, University of Cologne, Joseph-Stelzmann-Straße 52, D-50931 Cologne, Germany

[1]Corresponding author

Four L-glutamate neurotransmitter transporters, the three Na^+-dependent GLAST-1, GLT-1 and EAAC-1, and the Cl^--dependent EAAT-4, form a new family of structurally related integral plasma membrane proteins with different distribution in the central nervous system. They may have pivotal functions in the regulation of synaptic L-glutamate concentration during neurotransmission and are believed to prevent glutamate neurotoxicity. To investigate the specific physiological and pathophysiological role of the neuronal EAAC-1, which is also expressed in kidney and small intestine, we have generated two independent mouse lines lacking EAAC-1. *eaac-1*$^{-/-}$ mice develop dicarboxylic aminoaciduria. No neurodegeneration has been observed during a period of >12 months, but homozygous mutants display a significantly reduced spontaneous locomotor activity.

Keywords: behavioral abnormalities/deficient mice/dicarboxylic aminoaciduria/EAAC-1/glutamate neurotransmitter transporters

Introduction

Excitatory synapses are surrounded by powerful, high-affinity Na^+-dependent transporters for the neurotransmitter L-glutamate. These transporters terminate the action of this excitatory neurotransmitter in the central nervous system (CNS) by reducing the high L-glutamate concentration in the excitatory synapse after neurotransmission to that of the resting synapse. Four members of a new class of neurotransmitter membrane transporters have been discovered: GLAST-1 (Storck *et al.*, 1992), GLT-1 (Pines *et al.*, 1992), EAAC-1 (Kanai and Hediger, 1992) and EAAT-4 (Fairman *et al.*, 1995).

The four transporters are glycoproteins with core proteins of 541, 521, 573 and 564 amino acid residues, with sequence identities between 50 and 55%. They have in common a very similar hydrophobicity pattern, but differ most strikingly in their tissue distribution. The glial transporter GLAST-1 was localized by *in situ* hybridization and immunochemistry in the oligodendrocyte-related Bergmann glia cells surrounding the Purkinje cell layer, the hippocampus and throughout the cortex (Storck *et al.*, 1992; Rothstein *et al.*, 1994). GLT-1 mRNAs were found in astrocytes (Lehre *et al.*, 1995) and GLT-1 proteins have been detected only in glial cells of brain (Danbolt *et al.*, 1992; Pines *et al.*, 1992; Rothstein *et al.*, 1994). EAAT-4 expression has been shown in cerebellum and placenta by Northern blot hybridization analysis. Polymerase chain reaction (PCR)-based assays indicated that EAAT-4 is expressed at low levels in brain stem, cortex and hippocampus (Fairman *et al.*, 1995). EAAC-1 is expressed in neurons such as pyramidal cells of the CA2–CA4 regions of the hippocampus, the dentate gyrus, the granular layer of cerebellum and the cerebral cortical layers II–IV (Kanai and Hediger, 1992; Rothstein *et al.*, 1994), but also strongly in peripheral tissues including kidney, intestine, heart and muscle (Kanai and Hediger, 1992; Mukainaka *et al.*, 1995).

The plasticity of the glutamatergic synapse is regulated on three levels: by exocytotic, presynaptic neurotransmitter release, receptor density at the postsynaptic membrane and by powerful neurotransmitter uptake systems. Regulation of the neurotransmitter concentration in the synaptic cleft is of critical importance, particularly as part of the presynaptic mechanisms that induce long-term potentiation (LTP) of the glutamate-mediated synaptic transmission. Glutamate transporter activity is regulated in the short term by protein kinase C (Casado *et al.*, 1993; Dowd and Robinson, 1996), arachidonic acid (Lundy and McBean, 1995; Trotti *et al.*, 1995; Zerangue *et al.*, 1995) and nitroxide (Pogun *et al.*, 1994; Volterra *et al.*, 1994). Regulated expression of the GLAST-1, GLT-1, EAAC-1 and EAAT-4 genes very likely controls synaptic transmission in the long term by adjusting the density of glutamate transporters at glutamatergic synapses.

Neurons are destroyed by sustained exposure to high levels of glutamate (Lucas and Newhouse, 1957; Olney and Sharpe, 1969; Olney *et al.*, 1971). Several recent reports suggested a dysfunction of the glutamate uptake system in some neurodegenerative disorders. A decreased capacity for the high-affinity Na^+-dependent glutamate uptake is believed to raise the synaptic glutamate concentration to excitotoxic levels, causing neuronal death. Whether the altered glutamate transport is a primary or secondary cause of neurodegeneration, e.g. in special forms of amyotrophic lateral sclerosis (Plaitakis and Caroscio, 1987; Rothstein *et al.*, 1992; Bensimon *et al.*, 1994), Huntington's disease (Olney and De Gubareff, 1978; Perry and Hansen, 1990) and Alzheimer's disease (Choi, 1988; Plaitakis *et al.*, 1988; Pomara *et al.*, 1992), is an open question.

To study the individual role of the three well-characterized members of the new family of Na^+-dependent, high-affinity membrane transporters *in vivo*, we have chosen the loss of structure and function approach.

We report here the generation and characterization of a mutant mouse line deficient in the neuronal EAAC-1

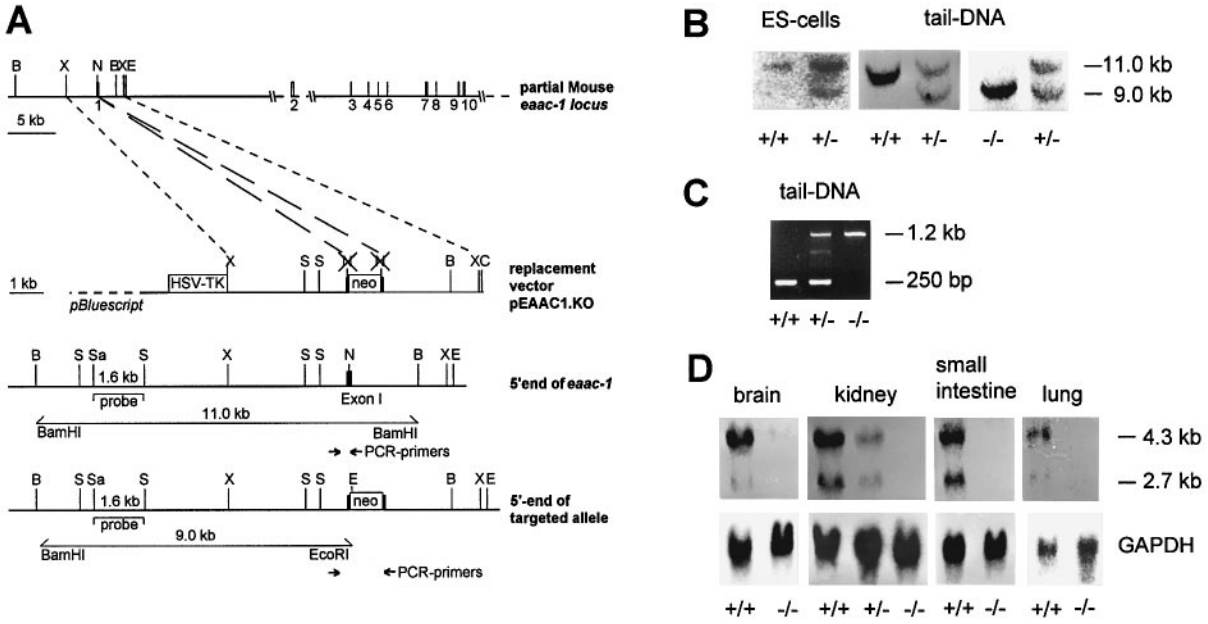

Fig. 1. Targeting of the *eaac1* locus by homologous recombination. (**A**) Organization of the *eaac-1* gene with partial restriction map (top), replacement vector pEAAC-1-KO for gene disruption (middle) and 5′ end of wild-type as well as targeted eaac1 allele (bottom). Exons are represented by solid bars, PGK-neo and PGK-tk by open rectangles. *Bam*HI/*Eco*RI double digest generates a 9 kb fragment from the targeted allele and an 11 kb fragment from the untargeted allele. Both are recognized by the 1.6 kb probe shown below the 5′ sequence outside the targeting vector. Positions of PCR primers are indicated by small arrows. The 5′ sense oligonucleotide primer (5′-CCGCCACGCAAAACCACCGTGCTCGGTCCC-3′) is located 150 bp upstream from ATG of exon 1 and the 3′ antisense primer (5′-CTAGTACCACGGCGGCCACGGTTGAGAGCA-3′) at the 3′ end of exon 1. The expected PCR fragments are 250 bp for the wild-type and 1.2 kb for the targeted allele. HSV-TK, thymidine kinase gene derived from herpes simplex virus linked to the phosphoglycerate kinase (PGK) promoter; neo, neomycin transferase gene linked to the PGK promoter. Restriction sites: B, *Bam*HI; E, *Eco*RI; N, *Nar*I; S, *Sst*I; Sa, *Sal*I; X, *Xba*I. (**B**) Southern blot analysis of genomic DNA extracted from ES cells and mouse tails. The DNA was digested with *Bam*HI and *Eco*RI, and hybridized with the probe. The sizes of wild-type (11.0 kb) and targeted (9.0 kb) alleles are indicated on the right, the genotypes of ES cells and mice below the lanes. (**C**) PCR analysis of tail genomic DNA extracted from mouse tails. Wild-type (250 bp) and mutant (1.2 kb) fragments were amplified using the set of primers described in (A). The genotypes of mice are indicated below the lanes. (**D**) Northern blot analysis of 40 μg of total RNA isolated from wild-type, hetero- and homozygous EAAC-1 mutants hybridized with a probe of rat EAAC-1 cDNA. Homozygous EAAC-1 mutants lack the 4.3 and 2.7 kb EAAC-1 mRNAs. GAPDH mRNA signals were used as an internal standard.

transporter. The wild-type transporter EAAC-1 gene was disrupted by homologous recombination with a mutant targeting construct.

Results

Isolation and partial characterization of the mouse EAAC-1 gene

Three mouse genomic EAAC-1 clones (M1–3) were isolated from a mouse genomic leukocyte library using a full-length EAAC-1 cDNA clone from a λgt10 rat brain cDNA library (W.Stoffel, unpublished data) and derived cDNA fragments. Eight exons and their flanking intron regions were sequenced. Exon sequences correspond to a previously published cDNA sequence of murine EAAC-1 (Mukainaka *et al.*, 1995). The partial gene structure of mouse EAAC-1 as far as relevant for the present study is shown in Figure 1A.

Targeted disruption of the mouse EAAC-1 gene

For gene targeting, the 7 kb *Xba*I fragment containing exon 1 flanked by 4 kb of genomic DNA on the 5′ and by 3 kb on the 3′ side was isolated and subcloned into pBluescript SKII+. Insertion of a pgk neomycin resistance gene cassette (neo) into the *Nar*I site disrupted exon 1 and served as a positive selection marker. The thymidine kinase gene was inserted 5′ of the genomic *Xba*I fragment for negative selection (Figure 1A). The resulting replacement vector (pEAAC-1.KO) was linearized with *Cla*I and introduced into R1 embryonic stem (ES) cells by electroporation. Transfected ES cells were subjected to negative/positive selection with G418 and gancyclovir. Resistant ES cell clones carrying the targeted allele were identified by Southern blot analysis of genomic DNA (Figure 1B). Positive ES cells were injected into C57BL/6 or CD1 blastocysts. Highly chimeric male animals were generated that transmitted the mutant allele to their offspring. *eaac-1*$^{+/-}$ mice were indistinguishable from wild-type animals. They were inbred and *eaac-1*$^{-/-}$ offspring were born at the predicted Mendelian ratio. The genotype of mice was determined by Southern blotting of mouse tail DNA restricted with *Eco*RI/*Bam*HI (Figure 1B) and PCR analysis (Figure 1C). The positions of the two oligonucleotide primers are marked in Figure 1A. They yielded a 250 bp PCR fragment with the wild-type DNA and a 1.2 kb fragment with the mutant template in which exon 1 is disrupted by the neo cassette. Two mouse lines were generated from different ES cell clones, one on the C57BL/6 (*eaac-1*$^{-/-}$.1) and one on the CD1 (*eaac-1*$^{-/-}$.2) background.

RNA from brain, kidney, small intestine and lung (Kanai and Hediger, 1992; Mukainaka *et al.*, 1995) from *eaac-1*$^{+/+}$, *eaac-1*$^{+/-}$ and *eaac-1*$^{-/-}$ mice was analyzed by Northern blot hybridization (Figure 1D). Consistent with

a previous report (Mukainaka *et al.*, 1995), two transcripts of different size (4.3 and 2.7 kb) were identified in brain, kidney, small intestine and lung of wild-type and heterozygous mice. Neither normal nor truncated mRNA could be detected in the tissues of *eaac-1*$^{-/-}$ mice.

Expression of EAAC-1 was detected by *in situ* hybridization of various brain regions (hippocampus, cerebellum and frontal cortex) in wild-type but not in *eaac-1*$^{-/-}$ mice (Figure 2).

We conclude that we have generated *eaac-1* null mice.

Phenotypic characterization

Mice homozygous for the disrupted *eaac-1*$^{-/-}$ allele developed normally. They were viable and fertile with normal mating efficiency. They have so far reached an age of >12 months with no apparent neurological disorder.

Brain, small intestine and kidneys are tissues with the highest *eaac-1* expression. We therefore examined the histology of these organs from wild-type and *eaac-1*$^{-/-}$ mice. Organ size and morphology at the cellular level were completely normal, and no differences were detected. Most importantly, hippocampus, cerebellum and cortex, regions of known high expression of *eaac-1*, showed an inconspicuous morphology and normal number of neurons (Figure 2).

eaac-1$^{-/-}$ *mice develop dicarboxylic aminoaciduria*. EAAC-1 is not brain specific, but is expressed very strongly in kidney and small intestine (Figure 1D). The function of EAAC-1 in tubular reabsorption of amino acids from the glomerular filtrate was studied by analyzing the amino acid pattern and concentrations of plasma and urine collected in metabolic cages from wild-type and EAAC-1-deficient mice over a period of 24 h. Quantitation of the amino acids present in the deproteinized urine by automated amino acid analysis revealed an increased excretion, 1400-fold for glutamate (240 nmol/g/24 h) and 10-fold for aspartate (5.6 nmol/g/24 h), in EAAC-1-deficient compared with wild-type mice (Figure 3). All other amino acids were present in comparable amounts, as were glutamate and aspartate in plasma of the two genotypes (*eaac-1*$^{+/+}$: glutamate 25 μM, aspartate 15 μM; *eaac-1*$^{-/-}$: glutamate 36 μM, aspartate 11 μM). These findings suggest that EAAC-1 specifically reabsorbs glutamate and aspartate in renal tubuli, and that other renal amino acid transporters do not compensate for the loss of its function in the EAAC-1-deficient mouse.

EAAC-1 deficiency does not induce upregulation of GLAST-1 and GLT-1. Northern and Western blot analyses revealed the low abundance of EAAC-1 in brain compared with the strong expression of the glial transporters GLAST-1 and GLT-1 (Rothstein *et al.*, 1994). Since the deficiency of the neuronal EAAC-1 in the *eaac-1*$^{-/-}$ mouse might upregulate the expression of the glial transporters, we monitored GLAST-1 and/or GLT-1 expression at the mRNA level by Northern blot hybridization analysis of total brain RNA. The signals in three repetitive experiments with different homozygous mice were quantified using a PhosphorImager (Molecular Dynamics) using the glyceraldehyde phosphate dehydrogenase (GAPDH) signal as internal standard (median value 98% GLAST-1 mRNA in *eaac-1*$^{-/-}$ compared with wild type, maximal difference 15%). An upregulation of GLAST-1 could clearly be excluded as its signal was equal in wild-type and *eaac-1*$^{-/-}$ mice. The values obtained for GLT-1 mRNA showed a large variation due to an incomplete transfer of this very large size mRNA (12 kb) from the gel to the nylon membrane.

We therefore applied reverse transcriptase (RT)–PCR with oligonucleotide primers for GLAST-1, GLT-1 and EAAC-1, and for GAPDH as unrelated template, to compare the concentrations of the individual glutamate transporter mRNAs (Gilliland *et al.*, 1990). Amplification was carried out for an increasing number of cycles using the oligonucleotide primers of the three transporters listed in Materials and methods and of GAPDH as control template (Figure 3).

The resulting PCR bands were quantified correlated to the internal GAPDH-control signal by the Image Quant program. No indication of an enhanced expression of GLAST-1 or GLT-1 in *eaac-1*$^{-/-}$ mice was observed in three repetitive experiments within the accuracy of the method.

eaac-1$^{-/-}$ *mice show no upregulation of GLAST-1 and GLT-1*. The peptide QYKTKREEVKPVGDP, corresponding to amino acid residues 161–175 of murine EAAC-1 (Mukainaka *et al.*, 1995), coupled to keyhole limpet hemocyanin (KLH) (Goodfriend *et al.*, 1964) was used as antigen for the immunization of rabbits. Antibodies were affinity purified on a Sepharose column derivatized covalently with the peptide listed above. The antibody titer was determined by ELISA (Engvall, 1980) using peptide coupled to bovine serum albumin (Reichlin, 1980).

Plasma membranes of brain of wild-type and mutant mice were isolated and proteins separated by PAGE (10% SDS). Western blot analysis was performed according to standard procedures (Sambrook *et al.*, 1989).

Figure 4 represents the Western blot analysis of wild-type and *eaac-1*$^{-/-}$ plasma membrane-enriched fractions of total brain. Equal amounts of protein were separated by 10% SDS–PAGE, proteins transferred by semi-dry blotting, and anti-GLAST-1 and -GLT-1 antibodies applied for the detection and estimation of GLAST-1 (70 kDa) and GLT-1 (73 kDa) proteins in wild-type and *eaac-1*$^{-/-}$ brains of the two phenotypes. The apparent equal intensity of the GLAST-1 and GLT-1 band (Figure 4) clearly demonstrates that no overexpression of the two glial transporter genes has occurred.

Mice lacking EAAC-1 show neither apoptosis nor reactive astroglia. Cryosections of brains of wild-type and *eaac-1*$^{-/-}$ mice were subjected to the TUNEL (TdT-mediated dUTP nick end labeling) reaction to verify cell apoptosis. Anti-glial acidic fibrillary protein (GAFP) antibodies were used to visualize potential astroglial reactivity. No differences between wild-type and mutant mice were observed (data not shown).

Neurological and behavioural assessment

Mice lacking EAAC-1 have normal motor coordination. Motor coordination of wild-type and EAAC-1-deficient mice was challenged in the rotating rod test. The time during which the mice were able to stay on a rod rotating at increasing speed (0.8, 1.6, 4, 8, 16 r.p.m.) was compared

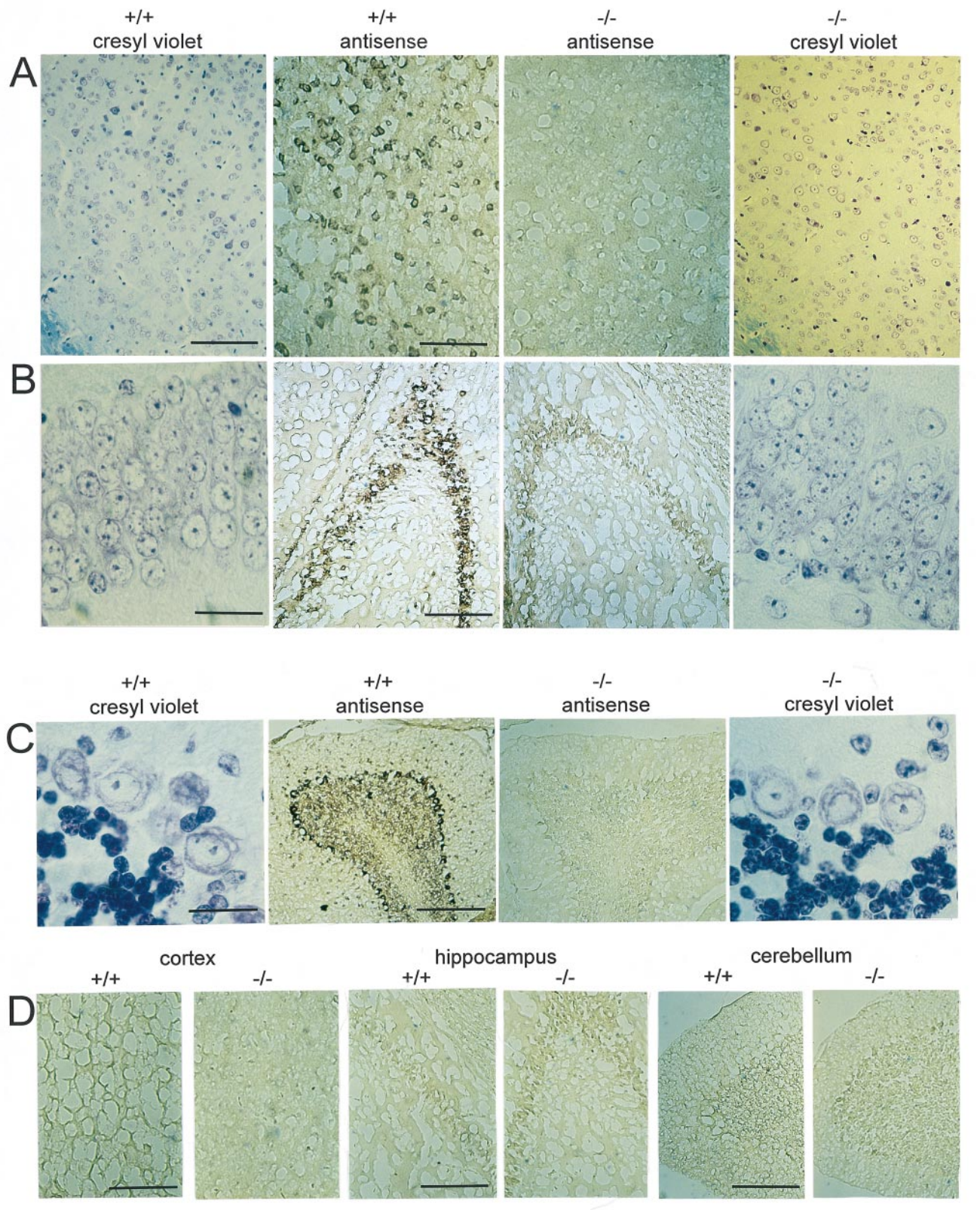

Fig. 2. *eaac-1*$^{-/-}$ mice show a normal histology of CNS. Sections from different brain regions from wild-type (left) and *eaac-1*$^{-/-}$ mice (right) were stained with cresyl violet. The complete loss of EAAC-1 mRNA in *eaac-1*$^{-/-}$ mice (middle, right column) is demonstrated by *in situ* hybridization using EAAC-1-specific antisense cRNA probes. Positively reacting sections of wild-type animals are shown for comparison (middle, left column). (**A**) Cerebral cortex: the number of cell bodies and organization in layers are equal in *eaac-1*$^{-/-}$ mice and controls. EAAC-1 expression is visible throughout the cortex in wild-type mice. Scale bar: 100 μm. (**B**) Hippocampal neurons of the two genotypes show normal appearance by number and morphology. EAAC-1 expression was observed in pyramidal cells of CA2–CA4 regions and in gyrus dentatus (latter not shown). Scale bar: 20 μm for cresyl violet-stained sections, 200 μm for *in situ* hybridizations. (**C**) Cerebellar Purkinje cell layer and adjacent structures are shown. No signs of neurodegeneration are visible (magnification ×1000). Note the strong expression of EAAC-1 in Purkinje cells and a weaker signal in stratum granulosum. Scale bar: 20 μm for cresyl violet-stained sections, 200 μm for *in situ* hybridizations. (**D**) Sections from the corresponding regions are shown for wild-type and *eaac-1*$^{-/-}$ mice that were hybridized with labeled sense probe as a negative control. Scale bar: 200 μm.

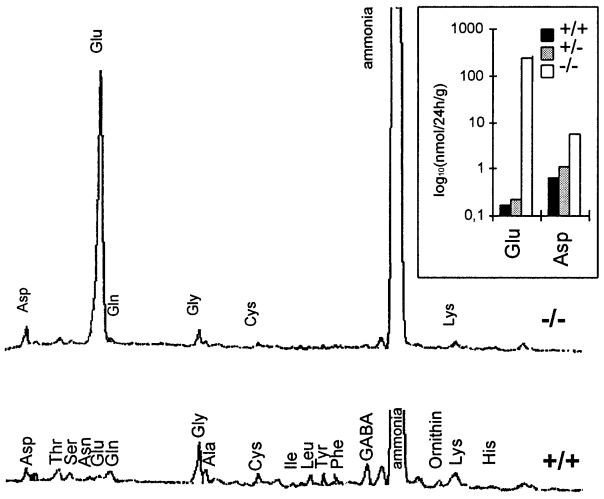

Fig. 3. Dicarboxylic aminoaciduria was assayed by quantitative amino acid analysis of urine from wild-type mice, as well as hetero- and homozygous EAAC-1 mutants. Urine of five female mice in each group was collected during 24 h and deproteinized by sulfosalicylic acid. Aliquots were separated by cation-exchange chromatography in an automated amino acid analyzer. Top recording, *eaac-1*$^{-/-}$ mice; bottom, wild-type *eaac-1*$^{+/+}$. EAAC-1-deficient mice show a large peak for glutamate as well as a smaller one for aspartate. All other amino acids were below the sensitivity of the method, except for glycine, which was also present in the urine of wild-type mice in considerable amounts. The inset shows the urinary excretion of glutamate and aspartate per 24 h in relation to body weight on a logarithmic scale for wild-type (black), heterozygous (gray) and homozygous *eaac-1*$^{-/-}$ mutant mice (open bars). The excretion was elevated 1400-fold for glutamate and 10-fold for aspartate in *eaac-1*$^{-/-}$ compared with wild-type mice. The levels for heterozygous mice are comparable with those of wild-type animals.

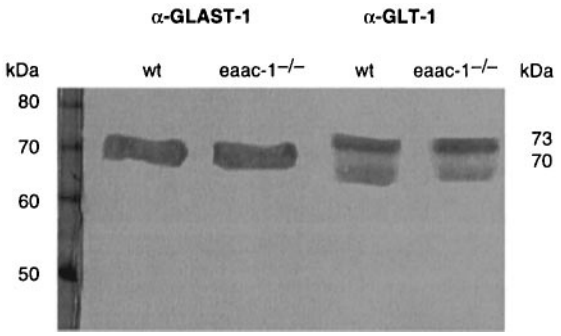

Fig. 4. Western blot analysis of plasma membrane fractions from wild-type and *eaac-1*$^{-/-}$ brains. Anti-GLAST-1 and -GLT-1 peptide antibodies were used for Western blot analysis. Distinct bands appeared around 70 and 73 kDa detecting GLAST-1 and GLT-1, respectively, in apparently identical concentrations.

for male *eaac-1*$^{-/-}$ mice from both lines, as well as for wild-type males of both strains (CD1 and C57BL/6). Motor coordination of *eaac-1*$^{-/-}$ and wild-type mice was indistinguishable. The differences between different wild-type strains were much larger than those between EAAC-1-deficient mice and their respective controls (Figure 6A).

Lack of EAAC-1 decreases spontaneous locomotor activity. The spontaneous locomotor activity of the wild-type and mutant mice at p35 was monitored in an open field chamber. The total number of squares crossed by male *eaac-1*$^{-/-}$ and wild-type mice during the observation on 3 consecutive days is depicted in Figure 6B. *eaac-1*$^{-/-}$ mice developed about half the locomotor activity of wild-type mice. This was not due to any overt neurological impairment such as pareses of fore- or hindlimbs or signs of ataxia. Homozygous mutants, however, discontinued their locomotion more frequently and for longer periods of time.

Spatial orientation in Morris water maze in EAAC-1-deficient mice is unimpaired. The Morris water maze task challenges locomotion, learning and memory of mice (Van der Staay *et al.*, 1992). Mice were challenged to find a platform situated below the water surface of a pool. The time they need to reach the platform decreases over a number of trials, and this decrease is a measure for their learning ability and spatial orientation. The differences observed did not reach statistical significance. The *eaac-1*$^{-/-}$.1 mice performed better and the *eaac-1*$^{-/-}$.2 line slightly worse than the respective control. In summary, the lack of function of EAAC-1 does not seem to impair learning in this spatial orientation task (Figure 6C).

Pentamethylenetetrazole-induced seizures. Pharmacological challenge with pentamethylenetetrazole (PTZ), a convulsant agent (Orloff *et al.*, 1949), revealed that the susceptibility of *eaac-1*$^{-/-}$ mice to seizures was comparable to the threshold of wild-type mice. A single i.p. injection of 75 mg/kg of PTZ produced the following sequence of events: after a latency period, the animals showed single whole-body twitches, followed by generalized clonic seizures, which sometimes progressed to a tonic stage with caudal extension of all four limbs and arrest of respiration, leading to death. Not all animals went through the whole sequence of events and recovery from every stage was possible, except for the tonic phase, which invariably led to death.

Mice from the *eaac1*$^{-/-}$.2 line ($n = 10$) were compared with wild-type animals derived from matings of heterozygotes ($n = 18$). The fractions of animals that reached different stages in the course of the epileptic reaction to PTZ are depicted in Figure 7A as a percent of the whole group. More animals of the *eaac1*$^{-/-}$ group died, but less reached the stage of convulsive seizures. The differences were statistically insignificant.

The average time that elapsed until different stages of the epileptic response to PTZ occurred is shown in Figure 7B. Animals that proceeded to later stages are included in the evaluation of the earlier stages. The time course was rather delayed in *eaac1*$^{-/-}$ animals, but the differences were statistically not significant ($P > 0.05$ in Student's *t*-test).

Discussion

Four glutamate transporters are believed to play an important role in neurotransmission at excitatory glutamatergic synapses. The individual contribution of the neuronal EAAC-1 and the three glial transporters, GLAST-1, GLT-1 and EAAT-4, in the regulation of the synaptic glutamate concentration is unknown and can hardly be deciphered by neurophysiological analyses because of the extensive overlapping of expression in different regions of the CNS, e.g. cerebellum, hippocampus, dentate gyrus, cortical cell layers and retina.

Here we report the first example of an *in vivo* analysis

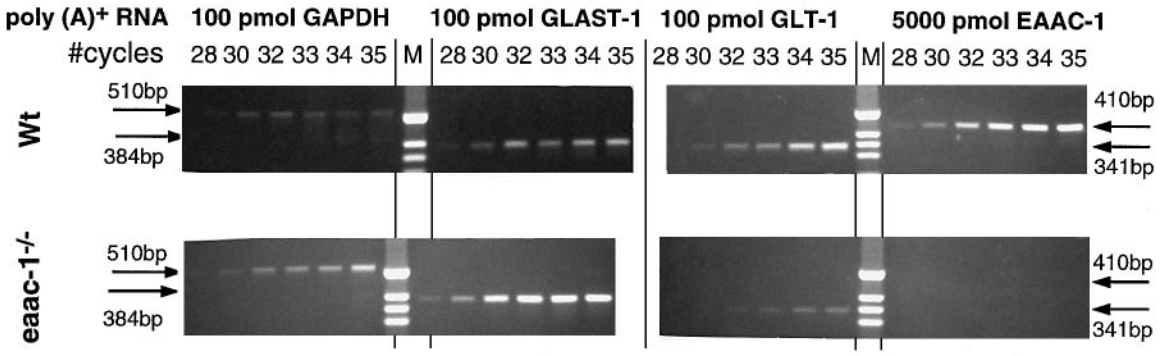

Fig. 5. RT–PCR of brain poly(A)$^+$ RNA of 3-month-old wild-type and *eaac-1*$^{-/-}$ mice. Amplification was carried out for the number of cycles indicated in the figure. Equal amounts of poly(A)$^+$ RNA were used for the RT–PCR with oligonucleotide primers probing for GAPDH, GLAST-1 and GLT-1. It is noteworthy that a 50-fold concentration of poly(A)$^+$ RNA was needed to achieve signal intensities comparable with those of the glial transporters. No signal was obtained with *eaac-1* primers in the knock out mouse.

of the function of an individual glutamate transporter, EAAC-1, within the synaptic machinery by studying allelic variations. The targeted disruption of the *eaac-1* gene, characterized here genetically and biochemically, has led to a loss of the EAAC-1 glutamate transporter system in the mouse.

eaac-1$^{-/-}$ *mice develop dicarboxylic aminoaciduria*

EAAC-1 is strongly expressed in kidney. The transporter is responsible for the tubular reabsorption of glutamate and aspartate from the glomerular filtrate. EAAC-1 deficiency leads to excessive glutamate and aspartate excretion by the kidney. The *eaac-1* locus has been mapped to chromosome 9p24 (Smith *et al.*, 1994). Mutations in the human EAAC-1 gene have been proposed as a cause for dicarboxylic aminoaciduria, an inborn error of glutamate/aspartate transport across epithelial cells of kidney and intestine that was associated with mental retardation in some cases (Teijema *et al.*, 1974; Swarna *et al.*, 1989), but with no neurological abnormalities in another one (Melançon *et al.*, 1977). Our mouse model, which carries a selective defect of EAAC-1, shows no neurological or cognitive abnormalities. Therefore, we conclude that the reported dicarboxylic aminoaciduria associated with mental retardation and athyreosis (Teijema *et al.*, 1974) probably represents a more complex hereditary or multifactorial defect.

Reduced spontaneous locomotion in eaac-1$^{-/-}$ *mice supports evidence for a role of glutamate in the regulation of motoric activity*

Three classes of glutamate receptors have been identified based upon their preference for one of three agonists: *N*-methyl-D-aspartate (NMDA), (*S*)-a-amino-3-hydroxy-5-methylisoxazole-4-propionic acid (AMPA) or quisqualate (Curtis and Watkins, 1960; Curtis and Johnston, 1974; Watkins and Evans, 1981; McLennan, 1983).The effects of glutamate and its agonists on the locomotor activity in rodents has been studied widely. Systemic administration of low doses of NMDA reduced motor activity, whereas higher systemically administered doses led to an initial motor depression followed by an increased motor activity (Von Lubitz *et al.*, 1993; Giménez-Llort *et al.*, 1995).

Intracerebral administration of quisqualate and AMPA to the nucleus caudatus and accumbens increased the locomotor activity (Shreve and Uretsky, 1988; Imperato *et al.*, 1990; Layer *et al.*, 1991; Burns *et al.*, 1994). Application of NMDA to the same areas enhanced locomotion only at high concentrations (Burns *et al.*, 1994). Injections of AMPA, but not NMDA, into the posterior zona incerta increased locomotion (Supko *et al.*, 1991). If these compounds were co-injected with amphetamine, which increases dopamine release and subsequently locomotion, quisqualate and AMPA enhanced the amphetamine-induced locomotor activity, whereas NMDA showed the opposite effect. This suppression of locomotor activity by NMDA was obtained with concentrations one order of magnitude lower than that required for a locomotion-stimulating response in co-injection experiments with quisqualate or AMPA and amphetamine (Burns *et al.*, 1994).

In summary, these observations not only indicate that the neurotransmitter glutamate modulates locomotion by acting at structures of the ventral striatum, but also that different glutamate receptors mediate different effects on locomotor activity. The precise site of administration, as well as the concentrations of glutamate agonists, seem to influence the response obtained. Excitatory synapses of the *eaac-1*$^{-/-}$ mouse are expected to have increased synaptic glutamate concentrations due to the deficiency of the neuronal uptake system. Three interpretations of the ~50% reduction in horizontal locomotor activity can be deduced from the experiments described above. First, among the glutamate agonists, only the administration of NMDA suppressed locomotion, whereas agonists at AMPA or quisqualate receptors always showed the opposite effect. Therefore, EAAC-1 may play a more important role at synapses harboring NMDA receptors than those with AMPA or quisqualate receptors. Secondly, considerably higher concentrations of AMPA and quisqualate agonists than of NMDA are required to produce specific changes in locomotor activity. The lack of EAAC-1 function may therefore lead to only very moderately increased glutamate concentrations which elicit an NMDA response inhibiting locomotion without activating AMPA and quisqualate receptors. Such an inhibitory response via glutamate receptors might be triggered either by depolarization blockade or feed-forward inhibition mediated by GABAergic neurons (Pennartz and Kitai, 1991; Burns *et al.*, 1994). As a third less likely possibility, the lack of an EAAC-1 reuptake system in the presynaptic membrane and, therefore, impaired recycling of the transmitter, may lead to a depletion of the presynaptic glutamate stores.

The cytosolic glutamate pool which is sustained by transamination of α-ketoglutarate and deamination of glutamine is, however, much larger than the vesicular store. It is the most likely source of the neurotransmitter in the glutamate vesicles which is predominantly replenished from the cytosolic pool rather than from recycling.

EAAC-1-deficient mice develop neither neurodegeneration nor epilepsy

Previous studies on the regional expression of *eaac-1* in CNS (Kanai and Hediger, 1992; Rothstein *et al.*, 1994) have demonstrated its expression in striatum, hippocampus, the granular and molecular layer, and Purkinje cells of cerebellum and throughout the cortex. Defective glutamate clearance by the transporters might lead to neurotoxic glutamate concentrations with excessive activation of postsynaptic glutamate receptors and neuron damage in these regions. A glutamate transporter defect has been proposed to cause neurodegenerative disorders such as amyotrophic lateral sclerosis (Rothstein *et al.*, 1992). A clinical trial showed a retarded progression of the disease by the glutamate antagonist riluzole, in patients with amyotrophic lateral sclerosis (Bensimon *et al.*, 1994). Further, glutamate-mediated neurotoxicity has been proposed as a possible cause of special forms of Huntington's disease (Olney and De Gubareff, 1978; Perry and Hansen, 1990) and Alzheimer's disease (Choi, 1988; Plaitakis *et al.*, 1988; Pomara *et al.*, 1992). Also, cerebral ischemia is associated with high extracellular glutamate concentrations leading to neuron death (Choi and Rothman, 1990; Nicholls and Attwell, 1990). One mechanism responsible for the high extracellular glutamate concentration induced by ischemia might be a presynaptic Ca^{2+}-induced glutamate release under hypoxic conditions. Another more likely mechanism might be the reversal of the electrogenic transporter system, as demonstrated in glial cells of salamander retina (Sarantis and Attwell, 1990; Szatkowski *et al.*, 1990). In tissue culture, astrocytes contribute much more than neurons to hypoxia-induced glutamate release (Ogata *et al.*, 1992). This emphasizes the importance of the glial transporter system compared with the glutamate release from presynaptic neurons.

Impaired glutamate transport may play a role in all of these conditions. Our work, however, shows that the lack of EAAC-1 alone is not sufficient to produce any histological or neurological changes associated with neurodegeneration.

Several lines of evidence point towards glutamatergic transmission as a pathogenic factor in epilepsy (for a review, see Meldrum, 1994). Local infusions of glutamate can cause seizures (Biscoe and Straughan, 1966), while glutamate receptor antagonists have anticonvulsant properties (Croucher *et al.*, 1982). Autoantibodies to glutamate receptor GluR3 have been shown to be the cause of Rasmussen's encephalitis, a progressive disease of childhood which is characterized by severe epilepsy and inflammation of the brain (Rogers *et al.*, 1994). These

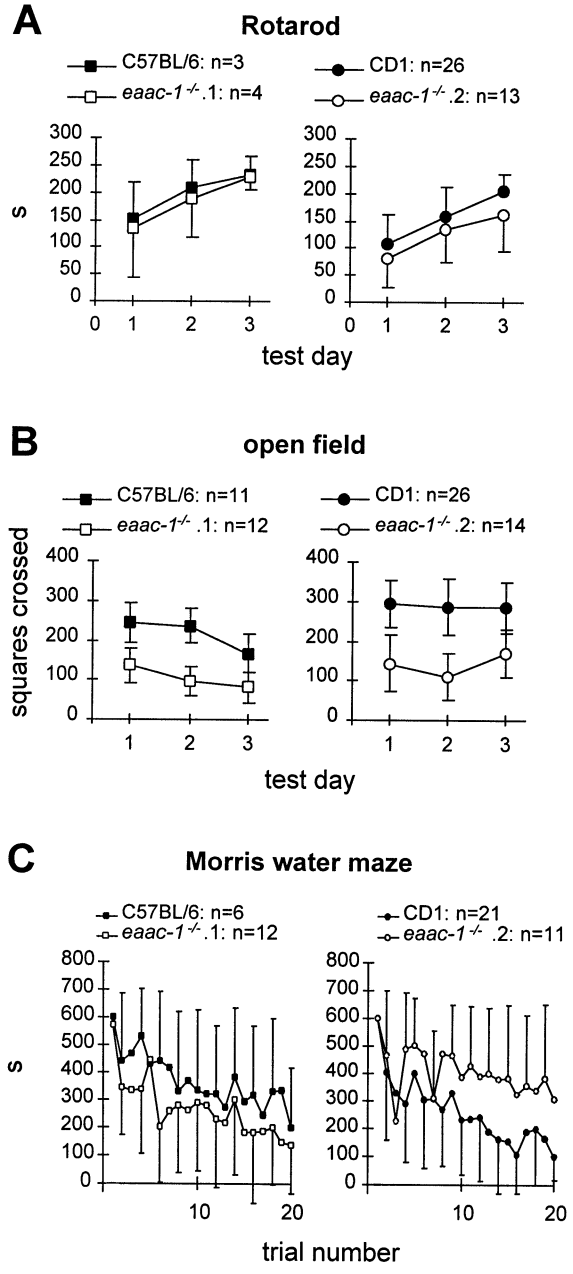

Fig. 6. Neurobehavioral assessment of *eaac-1*$^{-/-}$ mice discloses reduced locomotor activity, but no neurological or cognitive impairment. The groups of mice tested were *eaac1* null allelic mutants derived from C57BL/6 (*eaac-1*$^{-/-}$.1) or CD1 (*eaac-1*$^{-/-}$.2), as well as their respective wild-type strains C57BL/6 and CD1. For the sake of clarity, standard deviations are drawn in only one direction in (A) and (C). (**A**) *eaac-1*$^{-/-}$ mice show normal motoric coordination in the Rotarod test. The median time (s) that animals were able to stay on a rod rotating at increasing speed is shown for 3 test days. On each test day, three trials were carried out on each animal. Only small statistically insignificant differences were seen, as assessed by Student's *t*-test ($P = 0.08$–0.4). They were much smaller than differences between wild-type strains. (**B**) Spontaneous activity is markedly reduced in the open field test. The number of squares 10×10 cm that the animals crossed spontaneously in an open field box 60×60 cm during 5 min are drawn for three test sessions on consecutive days. *eaac-1*$^{-/-}$ mice of both null allelic lines showed a marked reduction in locomotion compared with wild-type control mice. The difference was statistically highly significant with $P < 0.01$ for all values. (**C**) Spatial orientation in the Morris water maze is unimpaired. The median time (s) that the animals needed to find a platform, situated below the water surface of a pool 70 cm in diameter, is depicted for 20 trials. Four trials per session were carried out on 5 consecutive days. The better performance of the *eaac-1*$^{-/-}$.1 line and the worse performance of the *eaac-1*$^{-/-}$.2 line compared with control mice indicates that none of the statistically insignificant differences can be attributed to the loss of EAAC-1.

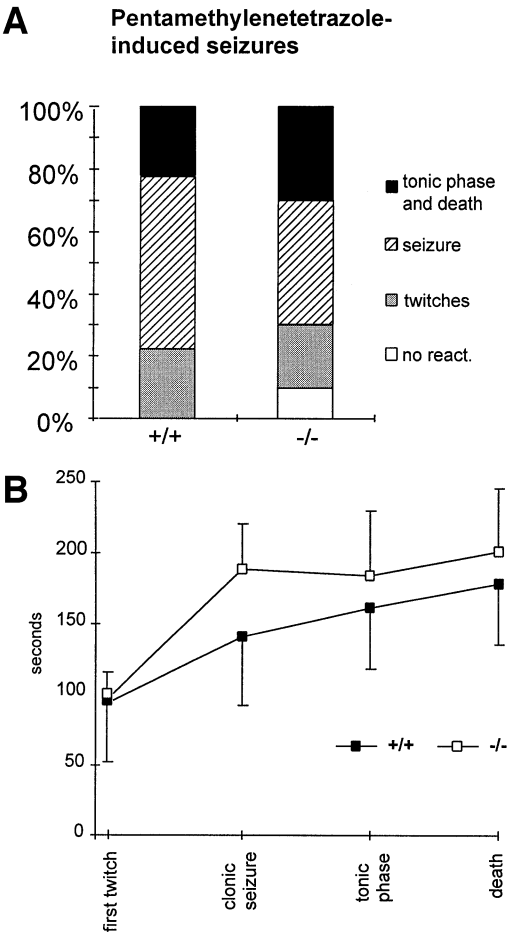

Fig. 7. Susceptibility to epileptic seizures induced by pentamethylenetetrazole (PTZ) in *eaac-1*$^{-/-}$ mice is not increased. Mice from the *eaac-1*$^{-/-}$.2 line ($n = 10$) were compared with wild-type animals derived from matings of heterozygotes ($n = 18$). (**A**) The fractions of animals that reached different stages in the course of the epileptic reaction to 75 mg/kg of PTZ are depicted as a percentage of the whole group. More animals died in the *eaac-1*$^{-/-}$ group, but less reached the convulsive seizure stage. (**B**) The average time that elapsed until different stages of the epileptic response to PTZ occurred is indicated in seconds. Animals that proceeded to a subsequent stage were included in the evaluation of the earlier stages. The time course was delayed in *eaac-1*$^{-/-}$ animals, but the differences were statistically insignificant ($P > 0.05$ in Student's *t*-test), except for the delay of clonic seizures ($P < 0.05$).

autoantibodies not only bind, but also activate GluR3, thereby leading to exaggerated excitatory neurotransmission and seizures (Twyman *et al.*, 1995). The excitatory neurotransmission mediated by glutamate seems to be controlled by the inhibitory effects of GABA. The rise of extracellular glutamate concentrations during epileptic seizures leads to a subsequent GABA release from neurons and the surrounding glial cells (During *et al.*, 1995). The balance between glutamate and GABA release seems to be disturbed in epileptogenic human hippocampi (During and Spencer, 1993).

The lack of EAAC-1 function was expected to lead to an increased synaptic glutamate concentration, an imbalance between glutamate and GABA, and an increased susceptibility to epileptic seizures. However, no spontaneous epileptic seizures have been observed in *eaac-1*$^{-/-}$ mice during a period of >9 months.

We therefore challenged a possible latent susceptibility to epilepsy of the *eaac-1*$^{-/-}$ mutants with the GABA antagonist PTZ. The susceptibility of the *eaac-1*$^{-/-}$ mouse after a single application of PTZ did not differ from that of age-matched wild-type mice.

A recent report describes an antisense oligonucleotide 'knock out' approach of neuronal *eaac-1* and of glial *glast-1* and *glt-1* expression (Rothstein *et al.*, 1996). Chronic intraventricular administration of the respective antisense oligonucleotides *in vivo* and to brain slices in culture led to a partial loss of functional glutamate transport activity of 35% for GLAST-1, 56% for GLT-1 and 22% for EAAC-1 antisense oligonucleotides. Mice with partial loss of functional EAAC-1 glutamate transport have been described to develop a motor syndrome with slow hind limb movement, atactic gait, hind limb paresis and, most notably, these mice produced epilepsy with clonic seizures. These findings are contradictory to the phenotype of the *eaac-1*$^{-/-}$ mouse described here.

We also investigated a possible apoptosis of neurons due to increased synaptic glutamate concentration using the *in situ* immunoperoxidase detection of digoxigenin-labeled genomic DNA of apoptotic cells (TUNEL assay) in cryosections. We were not able to detect any difference between wild-type and mutant mice. The same negative result to demonstrate astro-glial reactivity was obtained when anti-GAFP antibodies were applied to cryothin sections of wild-type and *eaac-1*$^{-/-}$ mice.

In summary, the EAAC-1-deficient mouse gives first insight into the relative role *in vivo* of the neuronal glutamate transporter. The expected neuropathological phenotype due to the EAAC-1 deficiency and a presumed elevation of synaptic glutamate concentration to toxic levels is missing in the hetero- and homozygous mutant. The inconspicuous phenotype of the homozygous *eaac-1*$^{-/-}$ mouse might result from a compensatory upregulation of the glial transporters GLAST-1 and GLT-1, or the existence of as yet unknown glutamate transporters, which take over the function of the neuronal EAAC-1 at the respective excitatory synapses. We exclude the glial EAAT-4 as a candidate which could compensate for the lack of EAAC-1 because the K_m is ~10 times lower than that of the other glial glutamate transporters (Fairman *et al.*, 1995). As a third possibility, EAAC-1 might have a function other than the stringent regulation of the synaptic glutamate concentration and, therefore, not be intimately related to the plasticity of glutamatergic synapses.

Our quantitative Northern blot analysis and radiolabeling RT–PCR make the first hypothesis very unlikely, as no enhanced expression of either GLAST-1 or GLT-1 was observed in the *eaac-1*$^{-/-}$ mouse within the limit of accuracy of these methods. In view of the low abundance of EAAC-1 mRNA and protein in the mouse brain, we question a vital function of EAAC-1 in the regulation of synaptic L-glutamate concentrations, unless other as yet unknown glutamate transporters compensate for the loss of EAAC-1 function in the null-allelic *eaac-1*$^{-/-}$ mouse. Therefore, the glial transporters may play the pivotal role in the neurotransmitter uptake system and also in preventing short- and long-term neurotoxicity.

Most current strategies that aim at the protection of neurons from post-ischemic and other glutamate overflow conditions and its neurotoxicity address the regulation of

the presynaptic glutamate release and the postsynaptic receptor systems. The glutamate transporter system might be a third target for manipulating the excitatory synapse. The *eaac-1*$^{-/-}$ mouse model, together with more *in vivo* information on the glial glutamate transporters, may prove valuable in developing strategies to regulate the synaptic glutamate concentration.

Materials and methods

Isolation of the mouse EAAC-1 gene

A λgt10 rat brain cDNA library (Storck *et al.*, 1992) was screened with a 642 bp PCR fragment that had been obtained using the 5′ pool primer AATCTGGTAGAAGCCTGCTTTAAACAG and the 3′ pool primer ACCATAACATGGATGGGACCGCCC. A full-length 2048 bp rat EAAC-1 cDNA clone was isolated. After radiolabeling, this rat EAAC-1 cDNA was used to screen a Balb/c mouse genomic library (Clontech ML1040j) (Sambrook *et al.*, 1989). Three overlapping genomic clones were isolated and the *eaac-1* organization was established by restriction mapping. Eight of the exons were sequenced.

The EAAC-1 targeting vector pEAAC-1KO contained a 7 kb *Xba*I restriction fragment of clone M3 with exon 1 flanked by 4 kb of genomic DNA on the 5′ side and 3 kb on the 3′ side. It was inserted into the *Xba*I restriction site of pBluescript SKII+. Exon 1 was disrupted by insertion of a pgk neomycin resistance gene cassette (neo) into an *Nar*I restriction site in sense orientation. A thymidine kinase expression box was inserted into the unique *Not*I site of the pBluescript SKII+ 5′ of the genomic fragment.

Generation and identification of ES cell clones and null-allelic mice

Mouse ES cells (R1 genotype, kindly provided by Dr A.Nagy, University of Toronto) were grown to 90% confluency on feeder layers of mitomycin C-treated G418-resistant mouse embryonic fibroblasts (Robertson, 1987). A total of 10^7 cells were electroporated with 20–30 μg of *Cla*I-linearized replacement vector DNA in 0.8 ml of phosphate-buffered saline (PBS) at 0°C in a 0.4 cm cuvette of a Bio-Rad gene pulser set at 220 V and 500 mF. After 24 h, transfected cells were selected in 300 or 400 μg/ml G418 and 2 mM gancyclovir. ES cell DNA was isolated from resistant clones after incubation for 12–15 h at 55°C in protein digestion buffer containing 1 mM EDTA, 50 mM Tris–HCl (pH 8.0), 20 mM NaCl, 1% SDS and 1 mg/ml proteinase K. Lysates were extracted with phenol–chloroform–isoamyl alcohol. DNA was precipitated with ethanol (20 mM sodium acetate) and resuspended in Tris–EDTA, digested with the restriction endonucleases *Eco*RI and *Bam*HI, and analyzed by gel electrophoresis in 0.5% agarose, followed by Southern blotting using a randomly ^{32}P-labeled 1.6 kb *Sal*I/*Sst*I probe from the region flanking the 5′ end of the genomic fragment. After hybridization, blots were washed and exposed to Kodak AR5 X-ray film for 48 h or scanned with a PhosphorImager (Molecular Dynamics). The expected size for mutant *eaac-1* (9 kb) was 2 kb less than that for wild type (11 kb) due to an *Eco*RI restriction site inserted with the neo box.

Blastocysts of C57BL/6 and CD1 females were injected with 10–25 cells of targeted clones, and groups of 5–14 blastocysts were transferred into pseudopregnant CD1 females as described (Bradley *et al.*, 1984; Hogan *et al.*, 1986). Chimeric male offspring were mated to C57BL/6 or CD1 females, according to the origin of the blastocysts. We monitored germline transmission of the injected ES cells by the inheritance of agouti coat color. Heterozygous and homozygous offspring were identified by Southern blotting, as described for ES cells, as well as PCR analysis of tail DNA. The positions of the two oligonucleotide primers were chosen to yield a 250 bp PCR fragment with the wild type and a 1.2 kb fragment with exon 1 disrupted by the neo cassette, for the mutant template.

RNA analysis

Northern blot analysis was carried out according to standard procedures (Sambrook *et al.*, 1989). Total RNA of 25- to 30-day-old mice was extracted from brain, kidney, small intestine and lung as described (Chomczynski and Sacchi, 1987). Forty micrograms of RNA were separated on 1% agarose/formaldehyde gels and blotted onto nylon membranes by capillary transfer using 20× SSC. Membranes were dried for 15 min at 80°C, wetted in 2× SSC and hybridized overnight at 42°C in 25% formamide, 1 M NaCl, 1% SDS, 5% dextran sulfate with a ^{32}P-labeled 1.0 kb *Nar*I probe (base 32–1079) from rat EAAC-1 cDNA. They were washed in 2× SSC, 1% SDS at 55–65°C. Radioactive signals on the membranes were detected using a PhosphorImager (Molecular Dynamics). GAPDH mRNA signals were used as internal standard to ensure the application of equal amounts of RNA.

For quantitative Northern blots, PhosphorImager signals were quantified by the Image Quant software (Molecular Dynamics). The results of different glutamate transporters were divided by the GAPDH signal of the same lane obtained by rehybridizing the blot with radiolabeled GAPDH probe.

Generation of antibodies and Western blot analysis

The peptide QYKTKREEVKPVGDP, corresponding to amino acid residues 161–175 of murine EAAC-1 (Mukainaka *et al.*, 1995), was coupled to KLH (Goodfriend *et al.*, 1964). A total of 200 μg of peptide/KLH in 250 μl PBS were homogenized with 250 μl complete Freund's adjuvant and a New Zealand white rabbit was immunized by i.m. injection. Booster injections were carried out in the same way with incomplete Freund's adjuvant at biweekly intervals. The rise of the antibody titer was monitored by ELISA (Engvall, 1980) using peptide coupled to bovine serum albumin (Reichlin, 1980). Serum was affinity purified on a Sepharose column with the above-mentioned peptide covalently linked.

Mice were killed by cranial dislocation and organs were removed, homogenized in 0.25 M sucrose and centrifuged at 800 *g* for 5 min to remove nuclei. Plasma membranes were then sedimented by centrifugation at 2500 *g* for 10 min, and the pellet was washed once in PBS and dissolved in electrophoresis sample buffer containing 10% SDS. Western blot analysis was performed according to standard procedures (Sambrook *et al.*, 1989).

An anti-GLT-1 peptide antibody was also kindly supplied by Dr B.Kanner, Hadassah Medical School, Jerusalem.

Comparative RT–PCR analysis

For comparative RT–PCR analysis of brain RNA of wild-type and *eaac-1*$^{-/-}$ mice for GLAST-1 and GLT-1 expression, the following RNA sense (s) and antisense (as) primers were used.

GLAST-1 (s): TCA ATG CCC TGG GCC TCG TTG T (m.p. 68°C)
(as): GGG TGG CAG AAC TTG AGG AGG (m.p. 68°C)

yielding a 384 bp fragment

GLT-1 (s): CCT CCA TCC GAG GAG GCC AAT (m.p. 68°C)
(as): CAG CTG CCT AGC AAC CAC TTC T (m.p. 68°C)

yielding a 341 bp fragment

GAPDH (s): GCC AAG GTC ATC CAT GAC AAC TT (m.p. 70°C)
(as): TTT CTT ACT CCT TGG AGG CCA TGT (m.p. 70°C)

yielding a 530 bp fragment

The reactions were carried out according to standard protocols (Kawasaki, 1990).

Tubes contained equal aliquots of RNA for RT reactions added at several dilutions. The PCR program included an initial denaturation at 94°C for 5 min, followed by 35 cycles with the following steps: denaturation at 94°C for 30 s, annealing at 60°C for 30 s, elongation at 72°C for 2 min. Using the Image Quant software program, relative intensities of the PCR fragments within the series were correlated with the fragment of the wild-type and the *eaac-1*$^{-/-}$ mouse.

In situ apoptosis detection

Cryosections (7 μm) of paraformaldehyde-perfused wild-type and *eaac-1*$^{-/-}$ mouse brains were subjected to the *in situ* apoptosis assay by direct immunoperoxidase detection of digoxigenin-labeled genomic DNA (TUNEL assay). The ApopTag *in situ* apoptosis detection kit (Oncor, Gaithersburg, MD) was used following the manufacturer's instructions.

In situ hybridization

Mice were killed and organs removed as described below under Histology. After post-fixation, organs were incubated three times for 5 min in PBS and dehydrated overnight in 0.5 M sucrose/PBS. They were embedded in an embedding medium for cryosections (OCT Compound 4583, Tissue-Tek), and 7 μm cryosections were cut.

For detection of EAAC-1 mRNA, the 642 bp mouse EAAC-1-specific PCR fragment (see the previous section: isolation of the mouse EAAC-1 gene) was labeled with digoxigenin-coupled UTP using the DIG RNA Labeling Kit (SP6/T7) (Boehringer Mannheim) according to the manufacturer's instructions and hybridized to EAAC-1 mRNA in brain sections. Bound probe was visualized with anti-digoxigenin antibodies and alkaline

phosphatase-coupled second antibodies using the DIG Nucleic Acid Detection Kit (Boehringer, Mannheim, following the manufacturer's instructions).

Histology

Mice were suffocated in CO_2 and intracardially perfused with 20 ml of 0.9% NaCl followed by 4% paraformaldehyde in PBS for 10 min. Brain, kidney and small intestine were removed and post-fixed overnight. Paraffin sections were stained with hematoxylin/eosin or cresyl violet (brain).

Amino acid analysis in plasma and urine

Urine was collected in metabolic cages. Blood was obtained by open cardiac puncturing after suffocating the animals in CO_2. Glutamate concentrations were quantitated on an automatic amino acid analyzer, Model Pharmacia LKB Alpha Plus, by cation-exchange chromatography.

Open field test

A box of 60×60×20 cm was used for open field tests. The bottom was divided into 10×10 cm squares. During the test session of 5 min, the pathway of the mouse was continuously plotted manually on an image of the open field. The number of squares crossed was counted for evaluation.

Rotarod test

The apparatus consisted of six compartments (30×15 cm), separated by walls 30 cm in height, that were crossed by a motor-driven rod 3 cm in diameter, mounted 20 cm above the floor. The compartments were charged with one mouse each. The speed of the rotating rod was increased every min from 0.8 r.p.m. initially to 1.6, 4, 8, and 16 r.p.m., and the total time a mouse was able to stay on the rod was recorded. Each mouse was given three trials on each of 3 consecutive days. Median values were calculated for each day.

Morris water maze

The maze consisted of a black pool 70 cm in diameter containing a black platform 7.5 cm in diameter situated 1.5 cm below the water surface and 10 cm from the border. A mouse was placed randomly into one of four sectors (north, east, south, west), and the time required to find the platform was recorded. Each animal was given four trials per test session on 5 consecutive days.

Pentamethylenetetrazole-induced seizures

C57BL/6- and CD1-derived homozygous *eaac-1*$^{-/-}$ mice (2 months old, weighing 18–20 g) and age-matched control mice with the same genetic background were housed in groups of up to 10 per cage in a room with a controlled light–dark cycle (12 h light/12 h dark) at 23°C with free access to laboratory chow and tap water. Mice received a single injection of 75 mg/kg at 2.5 mg/ml PTZ i.p. dissolved in PBS and were observed for 10 min.

Acknowledgements

The project was supported by grants from the BMBF, Interdisciplinary Center for Clinical Research Cologne (ZMMK), project 22, and by the Deutsche Forschungsgemeinschaft, Schwerpunkt 'Glia', Sto.32/34-1. P.P. is the recipient of a postdoctoral fellowship from the Swiss National Science Foundation. We thank Maria Düker, Rolf Müller and Berthold Gassen for their excellent technical assistance.

References

Bensimon,G., Lacomblez,L. and Meininger,V. (1994) A controlled trial of riluzole in amyotrophic lateral sclerosis. *N. Engl. J. Med.*, **330**, 585–591.

Biscoe,T.J. and Straughan,D.W. (1966) Micro-electrophoretic studies of neurons in the cat hippocampus. *J. Physiol.*, **183**, 341–359

Bradley,A., Evans,M., Kaufman,M. and Robertson,E. (1984) Formation of germ-line chimeras from embryo-derived teratocarcinoma cell lines. *Nature*, **309**, 255–256.

Burns,L.H., Everitt,B.J., Kelley,A.E. and Robbins,T.W. (1994) Glutamate–dopamine interactions in the ventral striatum: role in locomotor activity and responding with conditioned reinforcement. *Psychopharmacology*, **115**, 516–528.

Casado,M., Bendahan,A.S., Zafra,F., Danboldt,N.C., Aragon,C., Geminez,C. and Kanner,B.I. (1993) Phosphorylation and modulation of brain glutamate transporters by protein kinase C. *J. Biol. Chem.*, **268**, 27313–27317.

Choi,D.W. (1988) Glutamate neurotoxicity and diseases of the nervous system. *Neuron*, **1**, 623–634.

Choi,D.W. and Rothman,S.M. (1990) The role of glutamate neurotoxicity in hypoxic-ischemic neuronal death. *Annu. Rev. Neurosci.*, **13**, 171–182.

Chomczynski,P. and Sacchi,N. (1987) Single-step method of RNA isolation by acid guanidinium thiocyanate-phenol-chloroform extraction. *Anal. Biochem.*, **162**, 156–159.

Croucher,M.J., Collins,J.F. and Meldrum,B.S. (1982) Anticonvulsant actions of excitatory aminoacid antagonists. *Science*, **216**, 899–901.

Curtis,D.R. and Johnston,G.A.R. (1974) Amino acid transmitters in the mammalian central nervous system. *Ergeb. Biol. Chem. Exp. Pharmakol. Physiol.*, **69**, 97–188.

Curtis,D.R. and Watkins,J. (1960) The excitation and depression of spinal neurons by structurally related amino acids. *J. Neurochem.*, **6**, 117–141.

Danbolt,N., Storm-Mathisen,J. and Kanner,B.I. (1992) A (Na^+/K^+) coupled L-glutamate transporter purified from rat brain is located in glial cell processes. *Neuroscience*, **51**, 295–310.

Dowd,L.A. and Robinson,M.B. (1996) Rapid stimulation of EAAC-1-mediated Na+-dependent L-glutamate transport activity in C6 glioma cells by phorbol ester. *J. Neurochem.*, **67**, 508–516.

During,M.J. and Spencer,D.D. (1993) Extracellular hippocampal glutamate and spontaneous seizure in the conscious human brain. *Lancet*, **341**, 1607–1610.

During,M.J., Ryder,K.M. and Spencer,D.D. (1995) Hippocampal GABA transporter function in temporal-lobe epilepsy. *Nature*, **376**, 174–177.

Engvall,E. (1980) Enzyme immuno assay ELISA and EMIT. *Methods Enzymol.*, **70**, 419–439.

Fairman,W.A., Vandenberg,R.J., Arriza,J.L., Kavanaugh,M.P. and Amara,S.H. (1995) An excitatory amino-acid transporter with properties of ligand-gated chloride channel. *Nature*, **375**, 599–603.

Gavrieli,Y., Sherman,Y. and Ben-Sasson,S.A. (1992) Identification of programmed cell death *in situ* via specific labeling of nuclear DNA fragmentation. *J. Cell Biol.*, **119**, 493–501.

Gilliland,G., Perrin,S. and Bunn,H.F. (1990) Competitive PCR for quantitation of mRNA. In Innis,M.A., Gelfand,D.H., Sninsky,J.J. and White,T.J. (eds), *PCR Protocols*. Academic Press, Inc., San Diego, CA, pp. 60–69.

Giménez-Llort,L., Martinez,E. and Ferre,S. (1995) Dopamine-independent and adenosine-dependent mechanisms involved in the effects of *N*-methyl-D-aspartate on motor activity in mice. *Eur. J. Pharmacol.*, **6**, 171–177.

Goodfriend,T.L., Levine,L. and Fasman,G.D. (1964) Antibodies to bradykinin and angiotensin: A use of carbodiimide in immunology. *Science*, **144**, 1344–1346.

Hogan,B., Costantini,F. and Lacy,E. (1986) *Manipulating the Mouse Embryo*. Cold Spring Harbor Laboratory Press, Cold Spring Harbor, NY.

Imperato,A., Tage,H. and Jensen,L.H. (1990) Dopamine release in the nucleus caudatus and in the nucleus accumbens is under glutamatergic control through non-NMDA receptors: a study in freely moving rats. *Brain Res.*, **530**, 223–228.

Kanai,Y. and Hediger,M.A. (1992) Primary structure and functional characterization of a high-affinity glutamate transporter. *Nature*, **360**, 467–471.

Kawasaki,E.S. (1990) Amplification of RNA. In Innis,M.A., Gelfand,D.H., Sninsky,J.J. and White,T.J. (eds), *PCR Protocols*. Academic Press, Inc., San Diego, CA, pp. 21–27.

Layer,R.T., Uretsky,N.J. and Wallace,L.J. (1991) Effects of morphine in the nucleus accumbens on stimulant-induced locomotion. *Pharmacol. Biochem. Behav.*, **40**, 21–26.

Lehre,K.P., Levy,L.M., Ottersen,O.P., Storm-Mathisen,J. and Danbolt, N.C. (1995) Differential expression of two glial glutamate transporters in the rat brain: quantitative and immunocytochemical observations. *J. Neurosci.*, **15**, 1835–1853.

Lucas,D.R. and Newhouse,J.P. (1957) The toxic effect of sodium L-glutamate on the inner layers of the retina. *Arch. Ophthalmol.*, **58**, 193–201.

Lundy,D.F. and McBean,G.J. (1995) Pre-incubation of synaptosomes with arachidonic acid potentiates inhibition of (3H) D-aspartate transport. *Eur. J. Pharmacol.*, **291**, 273–279.

McLennan,H. (1983) Receptors for the excitatory amino acids in the mammalian central nervous system. *Neurobiology*, **20**, 251–271.

Melançon,S.B., Dallaire,L., Lemieex,B., Robitaille,P. and M.P. (1977) Dicarboxylic aminoaciduria: an inborn error of amino acid conservation. *J. Pediatr.*, **91**, 422–427.

Meldrum,B.S. (1994) The role of glutamate in epilepsy and other CNS disorders. *Neurology*, **44**(Suppl. 8), 14–23.

Mukainaka,Y., Tanaka,K., Hagiwara,T. and Wada,K. (1995) Molecular cloning of two glutamate transporter subtypes from mouse brain. *Biochim. Biophys. Acta*, **1224**, 233–237.

Nicholls,D. and Attwell,D. (1990) The release and uptake of excitatory amino acids. *Trends Pharmacol. Sci.*, **11**, 462–468.

Ogata,T., Nakamura,Y., Shibata,T. and Kataoka,K. (1992) Release of excitatory amino acids from cultured hippocampal astrocytes induced by a hypoxic-hypoglycemic stimulation. *J. Neurochem.*, **58**, 1957–1959.

Olney,J.W. and De Gubareff,T. (1978) Glutamate neurotoxicity and Huntington's chorea. *Nature*, **271**, 557–559.

Olney,J.W. and Sharpe,L.G. (1969) Brain lesions in an infant rhesus monkey treated with monosodium glutamate. *Science*, **166**, 386–388.

Olney,J.W., Ho,O.L. and Rhee,V. (1971) Cytotoxic effects of acidic and sulfur containing amino acids on the infant mouse central nervous system. *Exp. Brain Res.*, **14**, 61–70.

Orloff,M.J., Williams,H.L. and Pfeiffer,C.C. (1949) Timed intravenous infusion of metrazol and strychnine for testing anticonvulsant drugs. *Proc. Soc. Exp. Biol. Med.*, **70**, 254–257.

Pennartz,C.M.A. and Kitai,S.T. (1991) Hippocampal inputs to identified neurons in an *in vitro* slice preparation of the rat nucleus accumbens: evidence for feed-forward inhibition. *J. Neurosci.*, **11**, 2838–2847.

Perry,T. and Hansen,S. (1990) What excitotoxin kills striatal neurons in Huntington's disease? Clues from neurochemical studies. *Neurology*, **40**, 20–24.

Pines,G. *et al*. (1992) Cloning and expression of a rat brain L-glutamate transporter. *Nature*, **360**, 464–467.

Plaitakis,A. and Caroscio,J.T. (1987) Abnormal glutamate metabolism in amyotrophic lateral sclerosis. *Ann. Neurol.*, **22**, 575–579.

Plaitakis,A., Constantakakis,E. and Smith,J. (1988) The neuroexcitotoxic amino acids glutamate and aspartate are altered in the spinal cord and brain in amyotrophic lateral sclerosis. *Am. Neurol.*, **24**, 446–449.

Pogun,S., Dawson,V. and Kuhar,M.J. (1994) Nitric oxide inhibits 3H-glutamate transport in synaptosomes. *Synapse*, **18**, 21–26.

Pomara,N., Singh,R., Deptula,D., Chou,J., Schwartz,M. and LeWitt,P. (1992) Glutamate and other CSF amino acids in Alzheimer's disease. *Am. J. Psychiatry*, **149**, 251–254.

Reichlin,M. (1980) Use of glutaldehyde as coupling agent for proteins and peptides. *Methods Enzymol.*, **70**, 159–165.

Robertson,E.J. (1987) In Robertson,E.J. (ed.), *Teratocarcinomas and Embryonic Stem Cells: A Practical Approach*. IRL Press, Oxford, pp. 71–112.

Rogers,S.W., Andrews,P.I., Gahring,L.C., Whisenand,T., Cauley,K., Crain,B., Hughes,T.E., Heinemann,S.F. and McNamara,J.O. (1994) Autoantibodies to glutamate receptor GluR3 in Rasmussen's encephalitis. *Science*, **265**, 648–651.

Rothstein,J., Martin,L. and Kuncl,R. (1992) Decreased glutamate transport by the brain and spinal cord in amyotrophic lateral sclerosis. *N. Engl. J. Med.*, **326**, 1464–1468.

Rothstein,J., Martin,L., Levey,A., Dykes-Hoberg,M., Jin,L., Wu,D., Nash,N. and Kuncl,R. (1994) Localization of neuronal and glial glutamate transporters. *Neuron*, **13**, 713–725.

Rothstein,J.D. *et al*. (1996) Knockout of glutamate transporters reveals a major role for astroglial transport in excitotoxicity and clearance of glutamate. *Neuron*, **16**, 675–686.

Sambrook,J., Fritsch,E.F. and Maniatis,T. (1989) *Molecular Cloning. A Laboratory Manual*. 2nd edn. Cold Spring Harbor Laboratory Press, Cold Spring Harbor, NY.

Sarantis,M. and Attwell,D. (1990) Glutamate uptake in mammalian retinal glia is voltage- and potassium-dependent. *Brain Res.*, **516**, 322–325.

Shreve,P.E. and Uretsky,N.J. (1988) Role of Quisqualic acid receptors in the hypermotility response produced by the injection of AMPA into the nucleus accumbens. *Pharmacol. Biochem. Behav.*, **30**, 379–384.

Smith,C.P., Weremowicz,S., Kanai,Y., Stelzner,M., Morton,C.C. and Hediger,M.A. (1994) Assignment of the gene coding for the human high-affinity glutamate transporter EAAC-1 to 9p24: potential role in dicarboxylic aminoaciduria and neurodegenerative disorders. *Genomics*, **20**, 335–336.

Storck,T., Schulte,S., Hofmann,K. and Stoffel,W. (1992) Structure, expression and functional analysis of a Na^+-dependent glutamate/aspartate transporter from rat brain. *Proc. Natl Acad. Sci. USA*, **89**, 10955–10959.

Supko,D.E., Uretsky,N.J. and Wallace,L.J. (1991) Activation of AMPA/kainic acid glutamate receptors in the zona incerta stimulates locomotor activity. *Brain Res.*, **564**, 159–163.

Swarna,M., Rao,D.N. and Reddy,P.P. (1989) Dicarboxylic aminoaciduria associated with mental retardation. *Hum. Genet.*, **89**, 299–300.

Szatkowski,M., Barbour,B. and Attwell,D. (1990) Non-vesicular release of glutamate from glial cells by reversed electrogenic glutamate uptake. *Nature*, **348**, 443–446.

Teijema,H.L., van Gelderen,H.H., Giesberts,M.A.H. and Laurent de Angula,M. (1974) Dicarboxylic aminoaciduria: An inborn error of glutamate and aspartate transport with metabolic implications, in combination with a hyperprolinemia. *Metabolism*, **23**, 115–123.

Trotti,D., Volterra,A., Lehre,K.P., Rossi,D., Gjesdal,O., Racagni,G. and Danbolt,N.C. (1995) Arachidonic acid inhibits a purified and reconstituted glutamate transporter directly from the water phase and not via the phospholipid membrane. *J. Biol. Chem.*, **270**, 9890–9895.

Twyman,R.W., Gahring,L.C., Spiess,J. and Rogers,S.W. (1995) Glutamate receptor antibodies activate a subset of receptors and reveal an agonist binding site. *Neuron*, **14**, 755–762.

Van der Staay,F., Stollenwerk,A., Horvath,E. and Schuurman,T. (1992) Unilateral middle cerebral artery occlusion does not affect water-escape behavior of CFW1 mice. *Neurosci. Res. Commun.*, **11**, 11–18.

Volterra,A., Trotti,D., Floridi,S. and Racagni,G. (1994) Reactive oxygen inhibits high affinity glutamate uptake: Molecular mechanism and neuropathological implication. *Ann. NY Acad. Sci.*, **738**, 153–162.

Von Lubitz,D.K.J.E., Paul,I.A., Carter,M. and Jacobson,B.A. (1993) Effects of N^6-cyclopentyl adenosine and 8-cyclopentyldipropyl-xanthine on N-methyl-D-aspartate induced seizures in mice. *Eur. J. Pharmacol.*, **249**, 265–270.

Watkins,J.C. and Evans,R.H. (1981) Excitatory amino acid transmitters. *Annu. Rev. Pharmacol. Toxicol.*, **21**, 165–204.

Zerangue,N., Arriza,J.L., Amara,S.G. and Kavanaugh,M.P. (1995) Differential modulation of human glutamate transporter subtypes by arachidonic acid. *J. Biol. Chem.*, **270**, 6433–6435.

Received on January 2, 1997; revised on March 26, 1997